Application of X-ray Absorption Spectroscopy to the Studies of Structure and Bonding of Metal Complexes in Solution

TSUN K. SHAM

Chemistry Department, Brookhaven National Laboratory, Upton, New York 11973

Received August 7, 1985 (Revised Manuscript Received February 11, 1986)

X-ray absorption spectroscopy (XAS) deals with the measurement and interpretation of the X-ray absorption coefficients of characteristic absorption edges of elements in various environments. The absorption coefficient often exhibits oscillations extending to as much as 1000 eV above the threshold. These are the extended X-ray absorption fine structures (EXAFS).[1] In the last decade, EXAFS has developed to become a reliable tool for the determination of local structures.[2-8]

The Pt L_{III} absorption spectrum of $PtCl_4^{2-}$ in aqueous solution shown in Figure 1 illustrates the two regions of an XAS spectrum. For many purposes, an XAS spectrum can be divided in two regions.[9] The first ~50 eV above the edge is the near edge region, often called x-ray absorption near edge structure (XANES). XANES corresponds to the excitation of a core electron into a previously unoccupied state (such as a molecular orbital) or a resonance state (often called virtual molecular orbital or shape resonance).

EXAFS arises from the intereference of the outgoing photoelectron wave with itself when it gets backscattered by neighboring atoms in a molecule or in condensed matters (no neighboring atom, no EXAFS). The oscillatory behavior occurs when the backscattered wave interfers with the outgoing wave either constructively or destructively at the site of absorption (near the origin of the absorbing atom). The interference pattern depends on the wavelength of the electron, the nature of the absorbing and scattering atoms (characteristic phase ϕ and backscattering amplitude $f(k,\pi)$), the distance between the absorber and the scatterer (bond length r), and the dynamic behavior of the system (vibrational motion, the Debye–Waller-like factor or more accurately the root-mean-square relative displacement (RMSRD), σ_i. The change in X-ray energies varies the electron wavelength and results in the increase or decrease of the photoelectron wave function at the absorption site and hence the absorption. This is because the phase between the outgoing and the backscattered waves changes as the wavelength changes. Since photoelectrons have short mean free path in condensed matters, EXAFS is only sensitive to the local environment (generally $\lesssim$4 Å from the absorbing atom). Thus EXAFS is ideal for studying short range order in solution.

The experimental EXAFS function $\chi(k)$ can be described by the single-particle, single-scattering, short-range order theory.[2-6] The most interesting feature of this theory is the additivity of waves of absorbing-scattering atom pairs. If we consider only the first coordination shell of a random sample, the K edge EXAFS function is given approximately by

$$\chi(\mathrm{k}) = -\sum_i \frac{N_i}{kr_i^2}|f_i(k,\pi)|e^{-2\sigma_i^2k^2} \sin(2kr_i + \phi_i(k)) = \sum_i A_i(k) \sin \Phi_i(k) \quad (1)$$

Here k is the photoelectron wave vector, $k = [2m(h\nu - E_0)/\hbar^2]^{1/2}$, and N_i is the number of nearest neighbors (backscatterers) of the same kind. Other parameters have their usual meaning.[10] We can derive the local spatial structure r from sin $\Phi_i(k)$ N_i and σ_i of the absorbing atom using known phase ϕ_i and amplitude $|f_i(k,\pi)|$ functions.

The ability of XAS to solve structural problems in solution was demonstrated by several groups during the early development of synchrotron spectrometry.[11-14] In this Account, the application of XAS to metal complexes in solution is described in connection with the structural and electronic aspects of electron exchange reactions[15-17] and substitution reactions.[18] The fun-

Tsun K. Sham received his B.Sc. degree from the Chinese University of Hong Kong and his Ph.D. degree from the University of Western Ontario in 1975. After 1.5 years as a postdoctoral fellow at Western Ontario, he joined the Chemistry Department at Brookhaven National Laboratory where he now holds the position of Chemist. His current research has centered on the electronic properties of solids and surfaces and the development and application of synchrotron radiation spectroscopies.

(1) R. de L. Kronig, Z. Phys., 70, 317 (1931); 75, 191 (1932); 75, 468 (1932).
(2) E. A. Stern, Phys. Rev. B: Solid State 10, 3027 (1974).
(3) (a) D. E. Sayers, E. A. Stern, and F. W. Lytle, Phys. Rev. Lett., 27, 1204 (1971); (b) F. W. Lytle, D. E. Sayers, and E. A. Stern, Phys. Rev. B: Solid State, 11, 4825 (1975); (c) E. A. Stern, D. E. Sayers, and F. W. Lytle, ibid., 11, 4836 (1975).
(4) C. A. Ashley and S. Doniach, Phys. Rev. B: Solid State, 11, 1279 (1975).
(5) P. A. Lee and J. B. Pendry, Phys. Rev. B: Solid State, 11, 2795 (1975).
(6) P. A. Lee and G. Beni, Phys. Rev. B: Solid State, 15, 2862 (1977).
(7) "Synchrotron Radiation Research", H. Winick and S. Doniach, Eds.; Plenum Press: New York, 1980.
(8) "Handbook on Synchrotron Radiation", E. E. Koch, Ed., North-Holland Amsterdam, 1983; Vol. 1.
(9) "EXAFS and Near Edge Structure", A. Bianconi, L. Incoccia, and S. Stipcich, Eds., Springer-Verlag, New York, 1983. "EXAFS Near Edge Structure III", K. O. Hodgson, B. Hedman, and J. E. Penner-Hahn, Eds., Springer-Verlag, New York, 1984. These are the proceedings of two recent international conferences on the subject.
(10) The technique is now well established for general use; for a review see (a) S. P. Cramer and K. O. Hodgson, Prog. Inorg. Chem., 25, 1 (1979); (b) D. R. Sandstrom and F. W. Lytle, Annu. Rev. Phys. Chem., 30, 215 (1979); (c) B. K. Teo, Acc. Chem. Res., 13, 412 (1980); (d) P. A. Lee, P. H. Citrin, P. Eisenberger, and B. M. Kincaid, Rev. Mod. Phys., 53, 769 (1981).
(11) P. Eisenberger and B. M. Kincaid, Chem. Phys. Lett., 36, 134 (1975).
(12) D. R. Sandstrom, H. W. Dogen, and F. W. Lytle, J. Chem. Phys., 67, 473 (1977).
(13) A. Fontaine, P. Legarde, D. Raoux, M. P. Fontana, G. Maisano, P. Milgiliardo, and F. Wanderlingh, Phys. Rev. Lett., 41, 504 (1978).
(14) T. I. Morrison, A. H. Reis, Jr., G. S. Knapp, F. Y. Fradin, H. Chen, and T. E. Klippert, J. Am. Chem. Soc., 100, 2362 (1978).
(15) T. K. Sham, J. B. Hastings, and M. L. Perlman, J. Am. Chem. Soc., 102, 5904 (1980).

0001-4842/86/0119-0099$01.50/0

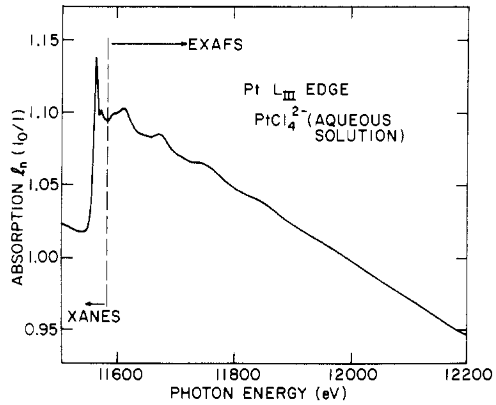

Figure 1. Pt L_{III} absorption spectrum of $PtCl_4^{2-}$ in aqueous solution.

damental understanding of these reactions is greatly facilitated by the quantitative information about the inner-shell configurations (bond lengths and RMSRD) of the metal complexes derived from EXAFS.[17] This information, which is usually obtained from crystal structure or X-ray and neutron diffraction techniques, is not readily available for most complexes in solution.

XAS spectra are usually recorded in a transmission mode in which the incoming (I_0) and the transmitted (I) photon flux are monitored with gas ionization chambers and the absorption is expressed as[7,8]

$$\mu(h\nu)t = \ln (I_0/I) \tag{2}$$

Several factors that affect the quality of the spectra are noted here. First, K edges should be used for EXAFS measurements whenever possible. For XANES studies of transition-metal complexes, L edges (L_{III}, L_{II}, and L_I) are most desirably.[19] Second, the thickness effect[20] that arises from sample nonuniformity, self-absorption, and higher order photons should be minimized.[10] Third, adequate resolution (<2 eV) is important for quantitative analysis of the amplitude. For dilute solution (concentration < 0.01 M), it is more desirable to record the data using fluorescence detection.[21]

EXAFS Data Analysis: Curve Fitting (CF) and Fourier Transform (FT)

Two methods are commonly employed concurrently in the analysis of EXAFS.[10] Chemical transferability is often assumed. The first step common to both is to convert the XAS spectrum (μt vs. $h\nu$) into EXAFS $\chi(k)$ with a k^n weighting.[22] The $\chi(k)k^2$ converted from Figure 1 is shown in Figure 2a which can already be analyzed by curve fitting to a model based on eq 1. It is however more desirable to do a FT analysis[10] which decomposes $\chi(k)k^n$ into a unique amplitude and phase

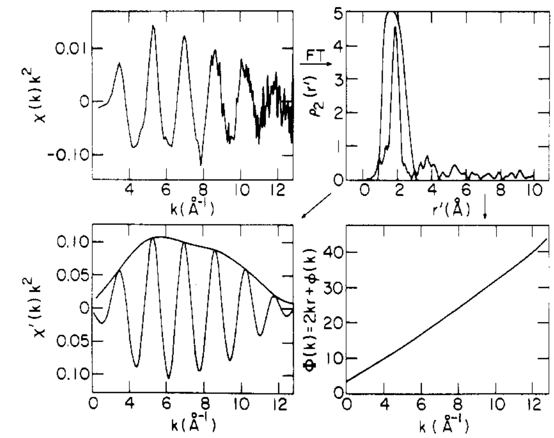

Figure 2. (a) EXAFS $\chi(k)k^2$ derived from Figure 1. (b) Fourier transform of (a). (c) Fourier-filtered and back-transformed EXAFS $\chi'(k)k^2$ that contains information concerning only the equatorial Pt–Cl bonds (the solid curve joining the maxima is the amplitude function (eq 4b)). (d) Experimentally derived phase function $\Phi(k) = 2kr_{Pt-Cl} + \phi(k)_{Pt-Cl}$.

function. The Fourier-filtered data containing the information of the Pt–Cl pairs are shown in Figure 2b–d. The filtered EXAFS $\chi'(k)$ (Figure 2c) can now be curve fitted to eq 1 by using known phase $\phi(k)$ and amplitude $f(\pi,k)$ functions from either theory or model compounds.[10] A scaling parameter $S(k)$ is often used in the analysis to account for the multielectron effect.[23] $S(k)$ is always less than unity. It should be noted that $S(k)$ is often not known very well and could vary considerably from compound to compound. This, together with the anharmonic vibration of the bond adds uncertainty to N_i and σ_i. In general, the accuracy of r_i, σ_i, and N_i amounts to ≤0.01 Å (0.05%), 10%, and 20%, respectively. This situation varies in solution depending on the stability of the complex but can often be improved by using chemically similar model compounds.

In situations where the difference in bond length (Δr) between two structurally closely related system is a desired parameter,[17,24,25] Δr can be accurately determined by fitting their phasse functions (Figure 2d, ΔE_0 is used as a parameter in the fit).[12] Since $\Phi(k)$ is linear in k for low Z backscatterers ($2kr > \phi(k)$, $\phi(k) = \alpha_1 + \alpha_2 k$, α_1 and α_2 being constant), one empirical rule for comparing bond lengths with EXAFS can be derived by considering the separation of adjacent maxima in $\chi(k)$ which is given by (from eq 1)

$$\Delta k_{max} = \pi/2(\alpha_1 r + \alpha_2) \tag{3}$$

On the basis of eq 3 where k_{max} is the position of the $\chi'(k)$ maxima, it can be generally stated that *for identical absorber–scatterer pairs of similar systems, the longer the bond, the closer the EXAFS oscillations in k space (hence energy space), and vice versa.*

Similarly, first shell coordination numbers and root-mean-square relative displacement of the atoms along the metal–ligand bond can be compared by considering the amplitude functions A_1 and A_2 of the two systems (Figure 2c; eq 4). By plotting $\ln (A_1/A_2)$ vs.

$$\ln\left(\frac{A_1}{A_2}\right) = \ln \frac{N_1 f_1(\pi,k)}{N_2 f_2(\pi,k)} \frac{r_2^2}{r_1^2} + 2(\sigma_2^2 - \sigma_1^2)k^2 \tag{4}$$

(16) T. K. Sham and B. S. Brunschwig, *J. Am. Chem. Soc.*, **103**, 1590 (1981).
(17) B. S. Brunschwig, C. Creutz, D. H. Macartney, T. K. Sham, and N. Sutin, *Faraday Discuss. Chem. Soc.*, **74**, 113 (1982).
(18) T. K. Sham, J. B. Hastings, and M. L. Perlman, *Chem. Phys. Lett.*, **83**, 391 (1981).
(19) M. Brown, R. E. Peierls, and E. A. Stern, *Phys. Rev. B: Solid State*, **15**, 738 (1977).
(20) E. A. Stern and K. Kim, *Phys. Rev. B: Solid State*, **23**, 3781 (1981).
(21) J. Jaklevic, T. A. Kirby, M. P. Klein, A. S. Robertson, G. S. Brown, and P. Eisenberger, *Solid State Commun.*, **23**, 679 (1977).
(22) The determination of χ is not straightforward since μ_0 is generally not known. A general procedure is to approximate μ_0 by a smooth curve (some polynomial or spline) fitted to μ. In transmission experiments, μ_0 drops off monotonically. In yield experiments in general μ_0 rises as a function of energy. See ref 10d for details.
(23) E. A. Stern, *Phys. Rev. Lett.*, **49**, 1353 (1982).
(24) N. Sutin, *Annu. Rev. Nucl. Sci.*, **12**, 296 (1962) and references therin.
(25) R. A. Marcus, *Annu. Rev. Nucl. Sci.*, **15**, 155 (1966).

Table I.
Parameters of Metal Ions in Aqueous Solution

aquo ion[a]	ionic radius[b] $r(M^{n+})$, Å	EXAFS bond length[c] $r(M-H_2O)$, Å	RMSRD,[c] $\sigma_i \pm 0.02$ Å	bond length (other techniques) $r(M-H_2O)$(solid), Å	bond length (other techniques) $r(M-H_2O)$(soln), Å	rate const k_1, s^{-1}
$Cr(H_2O)_6^{2+}$	0.80	eq 2.07 (1)	0.036			7×10^9
		ax 2.30 (5)	0.15			
$Cr(H_2O)_6^{3+}$	0.65	1.98	0.065	1.959 (3)[d]	1.98[i]	5×10^{-7}
$Mn(H_2O)_6^{2+}$	0.91	2.18	0.078	2.18[e]	2.20[g]	3×10^7
$Fe(H_2O)_6^{2+}$	0.83	2.10	0.081	2.123 (6)[f]	2.12[g]	3×10^6
				(1.96–2.15)[g]		
$Fe(H_2O)_6^{3+}$	0.67	1.98	0.055	1.995 (4)[d]	2.01[j]	3×10^3
$Co(H_2O)_6^{2+}$	0.82	2.05	0.082	2.08–2.23[h]	2.08,[g] 2.15[k]	1×10^6
$Ni(H_2O)_6^{2+}$	0.78	2.05	0.070	2.04–2.07[h]	2.04,[g] 2.05,[k] 2.07[l]	3×10^4
$Cu(H_2O)_6^{2+}$	0.72	eq 1.96(1)	0.036	1.97, 2.15[h]	1.94,[g] 2.15[k]	8×10^9
		ax 2.60(3)	0.12	2.31–2.80[b]	2.38,[g] 2.50[k]	

[a] Room-temperature measurements from ref 17 and 18 and unpublished results; the shorter axial distance in $Cr(H_2O)_6^{2+}$ reported in ref 18 was due to partial oxidation. [b] From ref 26, the total rate is the coordination number times k_1; SN_2 mechanism is responsible for the slow k_1 in $Cr(H_2O)_6^{3+}$. The bond length difference Δr for the $Fe(H_2O)_6^{2+/3+}$ couple is 0.13 Å from the phase-difference analysis; this value is used in the electron-exchange reaction analysis (Figure 4). [c] Uncertainty is ±0.01 Å unless indicated in the parentheses, or specified; error in σ_i is a very conservative estimate. [d] J. Baker, L. M. Engelhardt, B. N. Figgis, and A. H. White, *J. Chem. Soc., Dalton Trans.*, 530 (1975). [e] H. Montgomery, *Acta Crystallogr.*, **20**, 731 (1966). [f] J. Strouse, S. W. Layten, and C. E. Strouse, *J. Am. Chem. Soc.*, **99**, 562 (1977). [g] H. Ohtaki, T. Yamaguchi, and M. Maeda, *Bull. Chem. Soc. Jpn.*, **49**, 701 (1976). [h] References 1–20 in footnote g. [i] W. Bol and T. Welzen, *Chem. Phys. Lett.*, **49**, 189 (1977). [j] M. Magini, *J. Inorg. Nucl. Chem.*, **40**, 43 (1978). [k] I. M. Shapovalov, I. V. Radchenko, and M. K. Lesovitskaya, *Russ. J. Struct. (Engl. Transl.)*, **13**, 140 (1972); I. M. Shapovalov and I. V. Radchenko, *Russ. J. Struct. (Engl. Transl.)*, **12**, 769 (1971). [l] J. E. Enderby and G. W. Neilson, *Adv. Phys.*, **29**, 323 (1980).

k^2, we should get a straight line with a slope $2(\sigma_2^2 - \sigma_1^2)$ and an intercept, $\ln (N_1 r_2^2 / N_2 r_1^2)$. Such a comparison has been made for the $Fe(H_2O)_6^{3+/2+}$ system, both in the solid ($Fe(NO_3)_3 \cdot 9H_2O$ and $Fe(NH_4)_2(SO_4)_2 \cdot 6H_2O$ where $N = 6$) and in solution. The result indicates that within 5% accuracy these complexes remain six-coordinate in solution. This comparison does not work very well for dynamic systems like the Jahn–Teller ions.

Chemical Implication of EXAFS Parameters of Metal Ions in Solution

The implications of the EXAFS bond length and RMSRD are best illustrated with an EXAFS study of metal ions in aqueous solution and its correlation with the rate of water substitution reaction[26]

$$M(H_2O)_6^{n+} + H_2O^* \xrightarrow{k_1} M(H_2O)_5(H_2O^*)^{n+} + H_2O \tag{5}$$

where H_2O^* denotes the water molecule from the bulk and k_1 is the exchange rate constant. The difference in the rate constants among the metal ions is largely dependent upon their activation energy E_a[26] for dissociation which is closely related to the strength of the M–H_2O bond and hence the bond length and RMSRD.

A collection of EXAFS bond lengths and RMSRD for $M(H_2O)_6^{n+}$ ($n = 2, 3$) are given in Table I.[18] These ions can be divided into two classes: the octahedral and the tetragonally distorted (Jahn–Teller) $Cr(H_2O)_6^{2+}$ and $Cu(H_2O)_6^{2+}$ complexes. Let us consider the octahedral complexes for the moment. From Table I, several features are immediately evident. First the EXAFS bond lengths ($r(M-H_2O)$ are in general agreement with previous X-ray and neutron results[27] and tend to fall in the neighborhood of the lower limit of the crystal data. Second, among the octahedral M^{2+} aqueous ions, $Mn(H_2O)_6^{2+}$ (d^5, high spin) has the longest M–H_2O bond consistent with crystal field stabilization considerations.[26] Third, the RMSRD, σ_i, for 2+ ions are larger than those for 3+ ions. σ_i^2 in solution can be expressed as[14]

$$\sigma_i^2 = \sigma_{vib}^2 + \sigma_{stat}^2 + \sigma_{dyn}^2 \tag{6}$$

where σ_{vib}^2, σ_{stat}^2, and σ_{dyn}^2 are the mean-square relative displacement (MSRD) of the equilibrium M–H_2O distance resulting from all molecular vibration modes, static disorder, and inner-shell/outer-shell exchange involving first-shell H_2O and solvent H_2O molecules, respectively. In the limit of spherical screening of the octahedral complex by the solvent molecules, σ_{stat} (this may exceed 0.01 Å in the solid) vanishes. Further, σ_{dyn}^2 is variable depending on the nature of the system and its temperature but is small for strong M–H_2O bonds and slow ligand exchange. Therefore, in the context of the harmonic model, the MSRD σ_i^2 is a primary measure of the mean-square average of the displacement of the atoms from their equilibrium position in a particular bond, which is inversely proportional ot the square root of the force constant. One can therefore argue that, qualitatively, the bigger the σ_i the smaller the force constant and the weaker the bond. The fact that octahedral M^{2+} ions have larger r, bigger σ_i, and faster water exchange rate constants than M^{3+} ions is in qualitative accord with the S_N1 mechanism in which the rate-determining step requires a coordinated H_2O as a leaving group. The extremely slow rate for $Cr(H_2O)_6^{3+}$ indicates a different mechanism.[26]

It is interesting to compare the vibrational amplitude σ_{vib} with the root-mean-square relative displacement σ_i. Using the totally symmetric stretching mode of $Fe(H_2O)_6^{2+}$ ($\nu_s = 390$ cm^{-1}) and $Fe(H_2O)_6^{3+}$ ($\nu_s = 523$ cm^{-1}),[28] we can calculate the vibrational amplitude[29] (assuming harmonic motion) of the breathing motion of these complexes with

$$\sigma_s^2 = (h / 8\pi^2 \mu_M \nu_s) \coth (h\nu_s / 2kT) \tag{7}$$

(26) F. Basolo and R. G. Pearson, "Mechanism of Inorganic Reactions", Wiley, New York, 1967.
(27) See footnotes g and 1 of Table I. Also: Enderby, *Annu. Rev. Phys. Chem.*, **34**, 155 (1983).
(28) K. Nakamoto, "Infrared and Raman Spectra of Inorganic and Coordination Compounds", 3rd ed., Wiley, New York, 1978. The Fe^{3+} value was recently reported by S. P. Best, J. K. Beattie, and R. S. Armstrong, *J. Chem. Soc., Dalton Trans.*, 2611 (1984).
(29) S. J. Cyvin, "Molecular Vibrations and Mean Square Ampltiudes", Elsevier: Amsterdam, 1968.

Table II.
EXAFS Parameters[a] and Symmetric Breathing Amplitude of $Fe(H_2O)_6^{2+/3+}$ and $MnO_4^{-/2-}$

system	bond length		reorganization	RMSRD, σ_i	symmetric[c] breathing amplitude, σ_s, Å	
	reactant r, Å	activated[b] complex r^*, Å	$\lvert r^* - r \rvert$, Å		25 °C	100 °C
$Fe(H_2O)_6^{3+}$	1.98[d]	2.023	0.043	0.055	0.0187	0.0197
$Fe(H_2O)_6^{2+}$	2.10[d]	2.023	0.078	0.081	0.0233	0.0251
MnO_4^-	1.624	1.644	0.020	0.054	0.0180	0.0184
MnO_4^{2-}	1.666	1.644	0.022	0.056	0.0184	0.0188

[a] Uncertainty for r and σ_i is <0.01 Å for $MnO_4^{-/2-}$. [b] Values calculated on the basis of eq 12 and known frequency;[16,24,33] also see ref 16. [c] Values calculated on the basis of eq 7 and known frequencies.[16,24,33] [d] The bond length difference Δr of 0.13 Å was obtained from the phase-difference analysis. This value has been used in the electron-exchange reaction analysis (Figure 3).

where μ_M is the reduced mass and $h\nu_s$ is the photon energy ($\nu_s = \bar{\nu}_s c$, c = speed of light). The σ_s calculated for $Fe(H_2O)_6^{2+}$ and $Fe(H_2O)_6^{3+}$ at 25 °C from eq 7 are 0.0233 and 0.0187 Å, respectively. These values are small compared with the experimental σ_i's of 0.081 and 0.055 Å, respectively, for these two complexes, in qualitative accord with eq 6. Quantitatively however, the vibrational contribution of the normal modes does not seem large enough to account for σ_i. This discrepancy is most likely due to the inadequacy of the harmonic model as well as the uncertainty in the reduction of the EXAFS amplitudes ($S(k)$ and σ_{dyn}^2). More quantitative information can only be obtained from temperature-dependent measurements.

We now turn to the Jahn–Teller ions $Cr(H_2O)_6^{2+}$ and $Cu(H_2O)_6^{2+}$. This situation is particularly interesting because it not only involves two very different bond lengths within one complex but also shows the limitation of EXAFS in studying weak bonds. It has been shown that under these circumstances, the "weak bond" is not apparent in the Fourier transform, and more detailed modeling is needed for the extraction of the EXAFS parameters.[18] It turns out that the tetragonally distorted octahedron fits the data best.[18] It should be cautioned that while the EXAFS bond lengths of $Cr(H_2O)_6^{2+}$ and $Cu(H_2O)_6^{2+}$ are in close agreement with literature values, the σ_{ax} and σ_{eq} values have large certainty; their usage is at best qualitative. The position of the loosely bonded axial ligands can in principle be treated as a distribution in distance space ($e^{-\sigma^2 k^2}$ replaced by an integral).[10] Qualitatively, however, the observation is consistent with the interpretation that only axial ligands can be directly involved in the fast Cu^{2+} and Cr^{2+} water exchange.[26–28,30]

Application to Electron Exchange Reactions

Quantitative application of EXAFS parameters, particularly the bond length difference Δr is best found in the discussion of the rate of electron exchange reactions.[31,32] A typical electron exchange reaction for octahedral complexes can be expressed as[18,31]

$$ML_6^{2+} + ML_6^{3+} \xrightarrow{k_{obsd}} ML_6^{3+} + ML_6^{2+} \quad (8)$$

The rate of electron exchange can be understood in terms of a semiclassical model[31–33] in which the observed rate k_{obsd} is expressed as $K_A k_{el}$ where K_A is a preequilibrium constant and k_{el}, a first-order rate constant for electron transfer ($k_{el} = \nu_n \kappa_{el} \kappa_n$, the contribution of diffusion constant k_{diff}[31] is negligible). This model has been discussed elsewhere.[32,33] Here we only focus on the effects of the inner-shell configuration changes (κ_n) that greatly influence k_{el} (by 9 orders of magnitude). The effect of ν_n, the nuclear frequency, and κ_{el}, the electronic factor, will not be discussed.

The nuclear factor κ_n contains both solvent and inner-shell contributions.[17,33]

$$\kappa_n = \Gamma_\lambda \exp[-(\Delta G_{out}^* + \Delta G_{in}^*)/RT] \quad (9)$$

$$\Delta G_{out}^* = \left(\frac{\Delta q^2}{4}\right)\left(\frac{1}{2a_2} + \frac{1}{2a_3} - \frac{1}{d}\right)\left(\frac{1}{D_{op}} - \frac{1}{D_s}\right) \quad (10)$$

$$\Delta G_{in}^* = \frac{1}{2}\sum f_i[(\Delta r)_i/2]^2 \quad (11)$$

where Γ_λ is the nuclear tunnelling factor. ΔG_{out}^* and ΔG_{in}^* are the free energy of reorganization for the solvent and inner-shell contributions, respectively, Δq is the difference in charge between the two oxidation states, a_2 and a_3 are the radii of the two reactants (including coordinating ligands), $d = (a_2 + a_3)$, D_s and D_{op} are the static and optical dielectric constants of the medium, respectively, $f_i = 2f_2f_3/(f_2 - f_3)$ is a reduced force constant for the ith inner-sphere vibration, and $r_2 - r_3 = \Delta r$ is the bond length difference between the two oxidation states.

Let us consider for the moment the exchange rates in terms of the reorganization of the inner shells of the reactants in two systems $Fe(H_2O)_6^{2+}/Fe(H_2O)_6^{3+}$ and MnO_4^-/MnO_4^{2-}. Prior to electron transfer in these systems, an activated complex in which both reactants have rearranged their metal–ligand bonds to an identical bond length r^* must be formed. If we consider only the symmetrical breathing motion of the first (inner) coordination shell of the reactants, where one shell is compressed while the other is expanded, the common bond length r^* in the activated complex for the $Fe(H_2O)_6^{2+}/Fe(H_2O)_6^{3+}$ couple is given by

$$r^* = \frac{f_2 r_2 + f_3 r_3}{f_2 + f_3} \quad (12)$$

where f_2 and f_3 are the symmetric M–H_2O stretching force constants.[29] The results are listed in Table II together with EXAFS RMSRD and vibrational amplitudes calculated by using eq 7. It is apparent from Table II that the reorganization ($r - r^*$) for the $Fe(H_2O)_6^{2+}/Fe(H_2O)_6^{3+}$ (0.078 Å/0.043 Å) couple is much greater than ($r - r^*$) for the MnO_4^-/MnO_4^{2-} (0.020/0.022 A) couple. These values can be compared to the am-

(30) M. V. Eigen, *Ber. Bunsenges. Phys. Chem.*, 67, 753 (1963); R. Poupko and Z. Luz, *J. Chem. Phys.*, 37, 307 (1972).
(31) N. Sutin, *Acc. Chem. Res.*, 9, 275 (1982).
(32) M. D. Newton and N. Sutin, *Annu. Rev. Phys. Chem.*, 35, 437 (1984).
(33) B. S. Brunschwig, J. Logan, M. D. Newton, and N. Sutin, *J. Am. Chem. Soc. 102*, 5798 (1980).

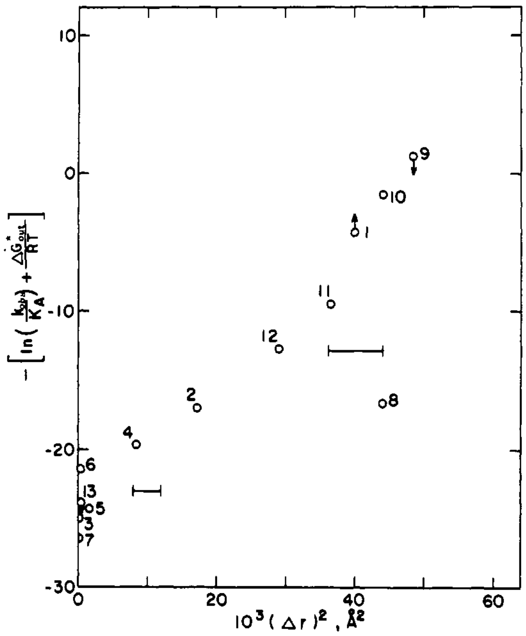

Figure 3. Correlation of the observed exchange rate constant (corrected for the stability of the precursor complex plus the outer-shell barrier divided by room temperature with $(\Delta r)^2$, the square of the difference of the metal–ligand bond distances in the two oxidation states:[17] (1) $Cr(H_2O)_6^{2+/3+}$; (2) $Fe(H_2O)_6^{2+/3+}$; (3) $Fe(phen)_3^{2+/3+}$; (4) $Ru(H_2O)_6^{2+/3+}$; (5) $Ru(NH_3)_6^{2+/3+}$; (6) $Ru(en)_3^{2+/3+}$; (7) $Ru(bpy)_3^{2+/3+}$; (8) $Co(H_2O)_6^{2+/3+}$; (9) $Co(NH_3)_6^{2+/3+}$; (10) $Co(en)_3^{2+/3+}$; (11) $Co(bpy)_3^{2+/3+}$; (12) $Co(sep)^{2+/3+}$; (13) $Co(bpy)_3^{1+/2+}$ (en = ethylenediamine; bpy = 2,2′-bipyridine; sep = "sepulchrate"; phen = 1,10-phenanthroline).

plitude (σ_s) of the total symmetric stretching (breathing) at room temperature. It can be seen that while σ_s for the $Fe(H_2O)_6^{2+}/Fe(H_2O)_6^{3+}$ couple is considerably smaller than the reorganization, σ_s for the MnO_4^-/MnO_4^{2-} couple is comparable to the reorganization, indicating that there is sufficient energy in the lower vibrational states in the latter system to supply the reorganizational energy even at room temperature while the former system requires higher vibrationally excited states. If ΔG_{in}^* in eq 9 is considered of major importance to the relative rate (this is often the case), the MnO_4^-/MnO_4^{2-} exchange should proceed faster than the $Fe(H_2O)_6^{2+}/Fe(H_2O)_6^{3+}$ exchange. This is indeed observed (k = 710 $M^{-1}\ s^{-1}$ for the former and k = 1.1 $M^{-1}\ s^{-1}$ for the latter).[24]

For a more quantiative analysis of the effect of Δr on the reaction rate, we can rearrange eq 9 to give

$$-\left[\ln\left(\frac{k_{obsd}}{K_A}\right)+\frac{\Delta G_{out}^*}{RT}\right]=\frac{\Delta G_{in}^*}{RT}-\ln(\kappa_{el}\nu_n) \quad (13)$$

where ΔG_{in}^* is a function of Δr^2 (eq 11). Brunschwig et al.[17] have studied a number of redox pairs and have shown that a good correlation exists between the exchange rate constant (corrected for the stability of the precursor complex and the outer-shell barrier) and Δr^2 from EXAFS as expressed in eq 13. The results[17] are plotted in Figure 3. It can be seen from Figure 3 that, with the exception of $Co(H_2O)_6^{2+/3+}$ which follows a different mechanism, the correlation is remarkably good.[32]

Near-Edge Structure and Bonding

The X-ray absorption near-edge structure (XANES)[34-36] probes the unoccupied density of states

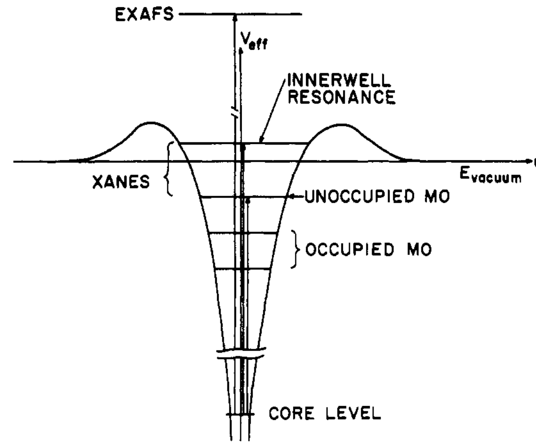

Figure 4. Schematics for the illustration of XANES. The potential barrier is responsible for resonance states in the continuum.

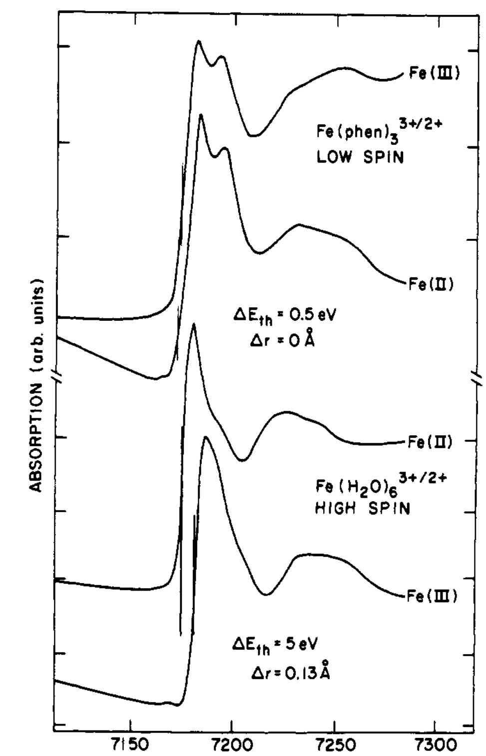

Figure 5. XANES of $Fe(H_2O)_6^{2+/3+}$ (weak π bonding) and $Fe(phen)_3^{2+/3+}$ (extensive π bonding). The E_{th} (marked with vertical bar) energy shift ΔE_{th} and bond length difference ($\Delta r = r_2 - r_3$ (derived from EXAFS analysis) are also given.

(bound and quasi-bound). A schematic of this situation in a metal complex is illustrated in Figure 4. The exact nature of the potential barrier depends on the chemical environment.[35,36] Our discussion here does not distinguish between states that are below the vacuum level or states just above the vacuum level. It should be noted that the position of the first peak (or the point of inflection of the rising edge E_{th}) merely corresponds to the excitation energy from the core level to the first

(34) W. H. Eugen Schwarz, *Angew. Chem.*, 13, 454 (1974).
(35) J. L. Dehmer, D. Dill, and A. C. Parr in "Photophysics and Photochemistry in the Vacuum Ultraviolet", S. P. McGlynn, G. Findley, and R. Huebner, Eds., D. Reidel, Dordrecht, 1984.
(36) T. K. Sham, *Phys. Rev. B: Solid State*, 31, 1888 (1985).
(37) J. P. Connerade, *Contemp. Phys.*, 19, 415 (1978).

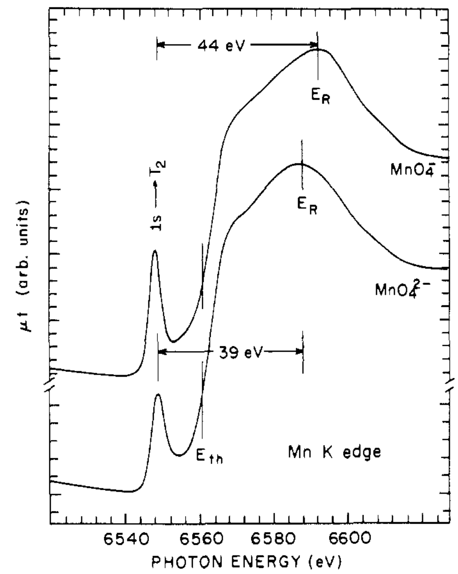

Figure 6. XANES of MnO_4^{2-} and MnO_4^- in solution (with moderate resolution). The position of the shape resonance E_R relative to the $1s \rightarrow T_2$ transition is given. E_{th} corresponds to the point of inflection of the rising edge. It can be seen that the closer the E_R to the threshold the longer the bond.

available, electric dipole allowed unoccupied state.

Although K edge absorption does not probe the d states directly, the XANES can still yield valuable information for chemically similar first-row transition-metal systems. Figure 5 shows the Fe K edge XANES of two Fe redox couples, $Fe(H_2O)_6^{2+/3+}$ and $Fe(phen)_3^{2+/3+}$, in solution. It can be seen that E_{th} shifts to higher binding energy from Fe(II) to Fe(III) in the high-spin aquo complexes as expected and is accompanied by a bond length decrease of 0.13 Å, whereas in the case of the low-spin pair, only a small edge shift and no EXAFS bond length difference is observed, indicating significant charge redistribution within the 1,10-phenanthroline complex resulting from extensive π bonding involving the ligand π orbitals and the metal d orbitals. It is also interesting to note that the small absorption feature below the edge jump arises from $1s \rightarrow 3d$ transition (dipole forbidden). Its amplitude depends on the occupancy and symmetry of the d states.

Under special circumstances, such as in the case of the MnO_4^-/MnO_4^{2-} couple in which the metal oxygen bond is extremely short, bond length information can even be obtained from the K edge XANES. It is now well established that the K edge XANES of simple molecules containing light elements (B to F) exhibit an intense shape resonance[38] which correlates with the interatomic distance in qualitatively the same manner as the EXAFS oscillations.[39] That is, *for chemically similar systems, the closer the shape resonance to the threshold the longer the bond.* Figure 6 shows the XANES of the MnO_4^-/MnO_4^{2-} couple. It can be seen that there is an intense shape resonance (this assignment is supported by the calculation by Kutzler et al.[40] for analogous CrO_4^{2-}) above the threshold. The shape resonance in the MnO_4^{2-} spectrum is closer to the threshold than that of MnO_4^-. This observation immediately indicates a longer Mn–O bond in MnO_4^{2-}. This procedure can be applied to chemically similar systems, particularly when the bonds are short. This is because a tight "cage" made up of the inner-shell ligands facilitates the "trapping" of the photoelectron long enough in the potential well.

Summary

We have presented the practice of X-ray absorption spectroscopy as applied to the study of structure and bonding of transition-metal complexes in solution and its correlation with chemical reactivity. It should be emphasized that *the ability to accurately determine bond length differences between closely related systems in solution such as the electron exchange pairs is a unique feature of EXAFS* and that bonding information can be infered from XANES. Because of its short-range sensitivity (<4 Å), XAS is proving itself to be very valuable for the investigation of local structure and bonding of a metal site in a large variety of chemical situations.

I am indebted to my colleagues Drs. B. Brunschwig, C. Creutz, J. Hastings, S. Heald, R. Holroyd, D. Macartney, M. Newton, M. Perlman, and N. Sutin for their collaboration, suggestions, and comments in various stages of the work discussed in this Account. I am particular grateful to the late Dr. Morris Perlman for his constant inspiration in the early stages of this work. EXAFS experiments were carried out at the Stanford Synchrotron Radiation Laboratory (SSRL) which is supported by DOE and at the Cornell High Energy Synchrotron source (CHESS) which is supported by NSF. Assistance of their staff is acknowledged. I also wish to thank the reviewer and the editor for their helpful comments. This research was carried out at Brookhaven National Laboratory under Contract DE-AC02-76CH00016 with the U.S. Department of Energy and supported by its Division of Chemical Sciences, Office of Basic Energy Sciences.

(38) A. P. Hitchcock, S. Beaulieu, T. Steel, J. Stöhr, and F. Sette, *J. Chem. Phys.*, **80**, 3927 (1984).
(39) Natoli in ref 9a, p 43.
(40) F. W. Kutzler, C. R. Natoli, D. K. Misemer, S. Doniach, and K. O. Hodgson, *J. Chem. Phys.*, **73**, 3274 (1980).